Volume 12, Number 3, 2019. pp. 269-289

Jordan Journal of Physics

ARTICLE

Discrimination of Aerosol Types over Nairobi, Skukuza and Ilorin Using AOD-AE Clusters

S. B. Sharafa[a], B. I. Tijjani[b], R. Aliyu[c], T. H. Darma[b], H. T. Sulu[d] and M. M. Bube[e]

[a] *Department of Physics, Usmanu Danfodiyo University Sokoto, Sokoto, Nigeria.*

[b] *Physics Department, Bayero University Kano, Kano, Nigeria.*

[c] *Physics Department, Kano State University of Science and Technology Wudil, Kano, Nigeria.*

[d] *Physics/Electronics Unit, Umaru Ali Shinkafi Polytechnic, Sokoto, Nigeria.*

[e] *Department of Management Information Systems, Usmanu Danfodiyo University Sokoto, Sokoto, Nigeria.*

Received on: 03/02/2019; *Accepted on: 9/9/2019*

Abstract: Climatology of aerosols, their trends and classification based on the long-term Moderate Resolution Imaging Spectroradiometer (MODIS) measurements (from February 2000 to July 2015) of aerosol optical depths at 550 nm (τ_{550}) and Angstrom exponent ($\alpha_{470\text{-}660}$) using the wavelengths of 470 and 660nm in Nairobi, Skukuza and Ilorin AERONET stations were analyzed in this work. The level-2 collection-6 Deep Blue (L2 C006 DB) of the parameters listed above from the aqua- (MYD04) and terra- (MOD04) MODIS of the study area were statistically analyzed using SPSS. To be able to understand the temporal variation in the characteristics of aerosols in the three stations and during each season separately, MODIS measurements of τ, retrieved for the study area, were compared with AERONET τ. Overall, aqua-MODIS τ corroborate the AERONET measurements well in Nairobi and Ilorin stations with underestimation of 29.80 % and overestimation of 2.90 % respectively, whereas Skukuza station has terra-MODIS τ as the best representation of the AERONET measurements with underestimation of 1.90 %. On seasonal bases, MODIS τ agree well with AERONET measurements during rainy season in Nairobi and Skukuza, with underestimation ranging between 17.20 % and 29.70 % and Ilorin station had overestimation of 7.20 % during dry seasons. Coupled with the fact that the coefficient of determination (R^2) > 0.50, the results suggest that both aqua- and terra-MODIS give a good estimate of τ. τ records presented a unique peak in Nairobi (June), Skukuza (October) and Ilorin (February), while the α monthly mean variability indicated a more complicated behavior with minimum values in Nairobi (June), Skukuza (June) and Ilorin (August). The maximum τ values occurred during dry seasons, while their minimum values occurred during rainy seasons or transition months. The α value showed an opposite behavior to that of τ such that the highest α values occurred during rainy seasons (or transition months) and the lowest values were observed during dry seasons. This behavior may be attributed to the domination of single-mode aerosol particles in each station. Lastly, τ and α values have been employed to identify several aerosol types seasonally and overall.

Keywords: Aerosol optical depth, Angstrom exponent, Terra and Aqua MODIS, AERONET, Validation, Discrimination.

Corresponding Author: S. B. Sharafa **Email**: sharafa.salihu@udusok.edu.ng

Introduction

Aerosol particles influence climate by modifying both the global energy balance through absorption and scattering of radiation (direct effects) and the reflectance and persistence of clouds and the development and occurrence of precipitation (indirect effects). The term “aerosol” denotes a stable, sparse suspension of microscopic or sub-microscopic solid and/or liquid particles in air. Aerosol particles contribute to numerous other climatically important processes, including fertilization of land and oceans through the deposition of nitrates, iron and other nutrients, acidification of lakes and forests through the deposition of sulfates and nitrates and the reduction of snow and ice albedo through the deposition of black carbon [1]. Reduction in the intensity of a direct solar beam during its propagation through the atmosphere is determined by absorption and scattering processes. These two different mechanisms contribute to extinction of light in the atmosphere from a directly transmitted beam [2].

The Moderate-resolution Imaging Spectroradiometer (MODIS) level II aerosol product (MOD04/MYD04) is the best aerosol optical depth product suitable for near-real-time aerosol data assimilation [3]. MODIS currently provides the most extensive aerosol retrievals on a global basis, but validation is limited to a small number of ground stations [4]. To validate the aerosol retrieval parameters, ground-based measurement data is necessary. The aerosol optical properties retrieved using direct solar radiations from the sun-photometers of the Aerosol Robotic Network (AERONET) are free from surface reflectance error and cloud contamination. Therefore, AERONET dataset is widely used to evaluate the efficiency of satellite based aerosol retrieval algorithm as well as to develop a new algorithm [5]. Several approaches have been proposed for the validation of MODIS aerosol retrieval algorithm for the purpose of renovating and improvement [6,7,8,9]. Kaufman *et al.*[9] proposed the first algorithm which was later modified by Levy *et al.*[10] and Hsu *et al.*[11] by proposing two different methods for aerosol retrieval.

To quantify the effect of atmospheric aerosols, it is necessary to increase our understanding of the subject by studying the spatial and temporal variability of its different properties [12]. Improvement in measurement capabilities of sensors has increased the amount of aerosol parameters retrieved from space-borne sensors. Several studies have demonstrated aerosol classification using various numbers of aerosol optical and physical parameters derived from passive satellite or ground-based measurements. For example, Kaufman *et al.*[13], Remer *et al.*[14] and Yu *et al.*[15,16] have used the aerosol size information contained in the wavelength dependence of τ retrieved from the space-borne MODIS to retrieve useful information on aerosol types and indeed to help distinguish natural from anthropogenic aerosols.

Discrimination of aerosol types is essential, because several aerosol types originate from different sources having different atmospheric impacts [17]. Aerosol discrimination based on τ_{550} and $\alpha_{470\text{-}660}$ scatter plot is useful in classifying different aerosols for a particular location through identifying and interpreting the level of density of τ_{550} and $\alpha_{470\text{-}660}$ (cluster) in the scatter diagram. The use of τ_{550} reveals the information about the aerosol density in an atmospheric column, while $\alpha_{470\text{-}660}$ gives information about aerosol size distributions. The τ_{550} and $\alpha_{470\text{-}660}$ values from the scatter plots can be interpreted together to identify the aerosol types and their frequencies in a particular location quantitatively. These, therefore, make regional studies important, because very different patterns in τ_{550} against $\alpha_{470\text{-}660}$ scatter plots have been observed by different authors from different regions of the world [18,19,20]. It is important to note that the $\alpha_{470\text{-}660}$ is commonly used due to its nearness to the peak of the solar spectrum and is thus associated with large radiative effect [12,21]. Granados-Munoz *et al.*[12] and Xin *et al.*[21] have used this angstrom values ($\alpha_{470\text{-}660}$) against τ_{550} to characterize and classify aerosols in different regions, because the two are indicative of turbidity condition and aerosol types.

The current study provides an attempt on the characterization of aerosols over AERONET stations in Nairobi (Kenya), Skukuza (South Africa) and Ilorin (Nigeria) using MODIS products for periods between the years 2000 and 2015. The study is based on two main objectives. The first is the validation of both aqua- and terra-MODIS τ_{550} with the same parameter from AERONET sensors, while the second is the utilization of τ_{550} and $\alpha_{470\text{-}660}$ climatology cluster analysis to discriminate aerosol types found in the study area over the same period using satellite data.

Data and Methodology

Study Location and Data Acquisition

The connection of two air masses, the impact of which varies during the year with the north–south displacement of the intertropical convergence zone (ITCZ) controls the climate in West Africa. During November–February, hot and dry continental air masses departing from the high-pressure system over the Sahara Desert offer ascent to dusty harmattan twists over the majority of West Africa. Moist central air masses which originate over the Atlantic Ocean bring annual rainfalls during the months from April to October [22]. The selected study location in West Africa is Ilorin (see Fig.1).

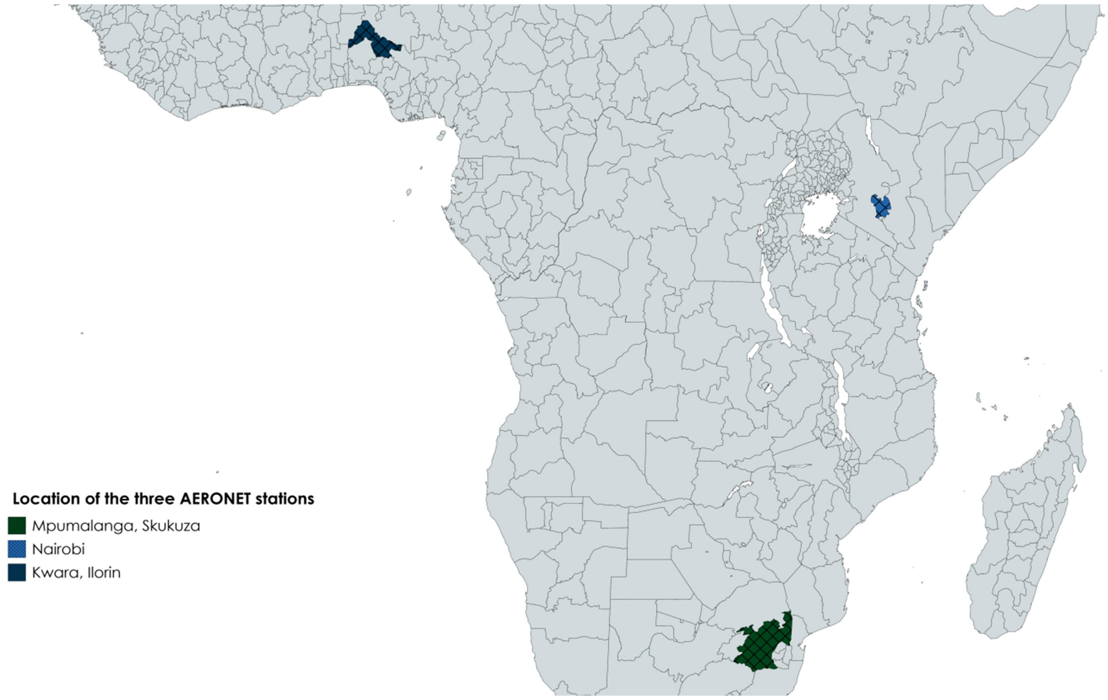

FIG. 1.The map of sub-Saharan Africa showing Skukuza, Nairobi and Ilorin.

East Africa covers different land forms that include glaciated mountains, semi-arid plateaus and coastal regions. The region also consists of inland plains together with forest covers which have been under threat of extinct in the recent past due to wood locking and deforestation. Moreover, the region experiences a distinct bimodal rainfall pattern; i.e., March-April-May (MAM) and September-October-November (SON) (wet season) characterized by low τ values due to enhanced scavenging of aerosols [23]. The bimodal rainfall pattern is influenced by the Inter Tropical Convergence Zone (ITCZ), global oceans, tropical high pressure systems, tropical Monsoons and cyclones [24]. On the contrary, high τ values are noted during dry season; i.e., December-January-February (DJF) and June-July-August (JJA). These high τ values are associated with enhanced aerosol emission from desert and biomass burning events with reduced scavenging of aerosols from the atmosphere through dry deposition. The selected study location in East Africa is Nairobi (see Fig.1).

The meteorological situation in South Africa is subject to a strong seasonal variability. Above the central Highveld, the atmospheric circulation pattern is dominated by anticyclonic circulation during winter and frequent easterly disturbances during summer. Westerly disturbances take place approximately 20% of the time throughout the year. The precipitation is characterized by strong seasonal variation with practically all precipitation falling during the wet season typically starting in October and ending in March. The precipitation cycle strongly affects local pollutant concentrations *via* primary emissions from wild fires during the dry season, as well as wet scavenging by precipitation and clouds during the wet season [25]. The selected study location in South Africa is Skukuza (see Fig.1).

The climate of the three stations under consideration is mainly characterized by two seasons; namely, dry and rainy. In addition, each station is influenced by various natural and anthropogenic aerosols due to the respective density of population and high pollution emission resulting in spatio-temporal variation [26]. The distribution of AERONET stations with level-2 data used for this work is shown in Table 1.

TABLE 1.Aeronet stations in the sub-Saharan Africa and their coordinates.

S/No.	Country	Aeronet station	Longitude	Latitude	Altitude	Rainy season	Region
1	Kenya	Nairobi	36°E	1°S	1650 m	March – May and Sept. – Nov.	East Africa
2	South Africa	Skukuza	31°E	24°S	150 m	October - April	South Africa
3	Nigeria	Ilorin	4°E	8°N	350 m	April - October	West Africa

MODIS

The Moderate Resolution Imaging Spectroradiometer (MODIS) is an instrument onboard NASAs Terra and Aqua satellites, which were launched in December 1999 and May 2002 [27], respectively. They are part of NASA's A-Train, a constellation of satellites that provide global daily coverage of the Earth's surface. The coordinated group of satellites allows for near-simultaneous observations of a wide variety of parameters to aid in understanding the Earth's climate. The A-Train is comprised of sun-synchronous near-polar orbiting satellites. Near-polar orbiting satellites pass nearly above the Earth's poles on each revolution and are synchronized with the sun, meaning that each successive orbital pass over the equator occurs at the same local time of the day and at a different longitude. The Terra satellite is on the descending orbit, crossing the equator at 10:30 a.m. local time and the Aqua satellite is on the ascending orbit, crossing the equator at 1:30 p.m. local time. Aqua and Terra fly approximately 700km above the Earth's surface and with MODIS having a scan angle of ±55°, MODIS views the Earth with an across-track swath of 2330 km and 10 km along-track. This allows for near global coverage on a daily basis with repeat orbits occurring every 16 days. MODIS is a radiometer that measures the spectral radiance reflected from the Earth-atmosphere system in 36 spectral bands or groups of wavelengths, from the solar to the thermal infrared (0.41μm -14.235μm).

Of the 36 spectral bands, the aerosol retrieval makes use of 7 bands in the shortwave and several others for cloud screening. Processing of the spectral reflectance (R_λ) for use in aerosol retrieval requires several steps. In each MODIS scan (2330 km across-track and 10 km along-track), there are approximately 1354 pixels with a 1 km channel resolution at nadir view. The number of pixels increases for higher resolution channels (250 m, 500 m). In order to process, the pixels are first averaged into 10 km^2 boxes with approximately 135 boxes per swath. Once averaged, R_λ are corrected for water vapor, ozone and carbon dioxide using ancillary datasets (MODIS atmospheric profile product (Level 2), allowing isolation of the aerosol signal. Following the correction, observations must be identified as cloudy or clear-sky. If identified as clear, the surface type is determined in order to account for differences in radiance reflection at the Earth's surface as well as differences in aerosol type. The boxes are screened for clouds using the MODIS cloud-mask (Level-2, 10 km^2 resolution) product. The cloud-mask product is also used for identification of the surface type. If any pixel within a 10 km^2 box is identified as land, the box is identified as land surface. Otherwise, a box is identified as ocean. Separate retrieval algorithms are used for ocean and land surfaces. A detailed description of pixel selection can be found in Remer *et al*. [14].

AERONET

The Aerosol Robotic Network (AERONET) is a network of approximately two hundred ground-based sun-photometers, which provide globally distributed and continuous observations of atmospheric aerosol properties (http://aeronet.gsfc.nasa.gov/) [28]. Observations are cloud-screened and include spectral aerosol optical depth (τ) and Angstrom exponents (α) as well as inversion products relating to aerosol size, such as aerosol optical depth due to fine aerosol and mean and standard deviation of the size distribution.

AERONET instruments measure the extinction of the direct solar beam in eight spectral bands; 340, 380, 440, 500, 670, 870, 940 and 1020 nm. Using the spectral extinction, the atmospheric optical depth is determined using the Beer-Lambert Law (Equation 1). Attenuation of the beam due to Rayleigh scattering and absorption by ozone and other gaseous pollutants is estimated and removed to isolate the aerosol optical depth. Measurements of aerosol optical depth by AERONET instruments are quite accurate because of the use of the direct solar beam. Possible offsets in solar channel calibration are expected to generate a wavelength-independent absolute uncertainty in AERONET τ at the level of ±0.01 [28]. This is more accurate than MODIS τ observations, which require information about surface reflectance properties that are not well quantified. As a result of low uncertainty, AERONET measurements are commonly used for validation of aerosol forecasts and satellite observations. In addition to τ, AERONET reports α, calculated using AERONET τ values for all available wavelengths (870,670, 500 and 440 nm).

$$I_\lambda = I_{\lambda 0} e^{-m\tau_{tot,}\lambda} \quad (1)$$

where I_λ is the observed spectral direct beam irradiance at wavelength λ, $I_{\lambda 0}$ is the extraterrestrial solar spectrum corrected for the actual Sun-Earth distance, m is the optical air mass and $\tau_{tot,}\lambda$ is the wavelength-dependent total optical depth (Kaskaoutis and Kambezidis, 2006; Masoumi et al., 2010 (as seen in Al-Salihi [29]).

Methodology

Aerosol Robotic Network (AERONET) and Moderate Resolution Imaging Spectroradiometer (MODIS) data was used in this work. The data was downloaded from the website of Multi-sensor Aerosol Products Sampling System (MAPSS) (http://giovanni.gsfc.nasa.gov/mapss/). It provides a consistent sampling approach that enables easy and direct inter-comparison and ground-based validation of the diverse aerosol products from different satellite sensors in a uniform and consistent way [30].

To characterize inconsistencies and bridge the gap that exists between aerosol sensors, MAPSS was established. The platform has consistently been sampling and generating the spatial statistics (mean, standard deviation, direction and rate of spatial variation and spatial correlation coefficient) of aerosol products from multiple spaceborne sensors, including MODIS (on Terra and Aqua), Multi-angle Imaging Spectroradiometer (MISR), Ozone Monitoring Instrument (OMI), Polarization and Directionality of Earth Reflectances (POLDER), Cloud Aerosol Lidar with Orthogonal Polarization (CALIOP) and Sea-viewing Field-of-view Sensor (SeaWiFS). Samples of satellite aerosol products are extracted over Aerosol Robotic Network (AERONET) locations as well as over other locations of interest, such as those with available ground-based aerosol observations. In this way, MAPSS enables a direct cross-characterization and data integration between Level-2 aerosol observations from multiple sensors. In addition, the available well-characterized co-located ground-based data provides the basis for the integrated validation of these products [30].

The simplest method to quantify the changes in spectral τ is to estimate Ångström parameters (α and β) using Eq. (2) [31,32,33],

$$\tau_{ext}(\lambda) = \beta \lambda^{-\alpha_{ext}} \quad (2)$$

τ is a measure of aerosol loading. Pure atmospheric conditions should be between 0.04 and 0.06 [34]. Ångström exponent (α) provides information on the aerosol size distribution, while the Ångström turbidity coefficient (β) is linked to the columnar mass loading of coarse-mode aerosols.

High α and low β indicate higher quantity of fine mode aerosol concentration. The α value depends on aerosol size distribution and varies from 1 to 3 for fresh and aged smoke and for urban aerosol particles, while it is nearly zero for coarse-mode aerosols, such as dust and sea salt [35]. α can be calculated using Eq. (3) [33,36,37]:

$$\alpha = -\frac{ln\left(\frac{\tau_1}{\tau_2}\right)}{ln\left(\frac{\lambda_1}{\lambda_2}\right)} \quad (3)$$

where τ_1 is the aerosol optical depth (AOD) at a reference wavelength λ_1 and τ_2 is the AOD at another wavelength λ_2.

Data Collection

For the purpose of this long-term analysis, the stations were selected purely based on the availability of an extensive data record. Specifically, calculation of the monthly mean of the parameters (both from AERONET and MODIS) using all-point measurements was carried out. A monthly mean was considered valid only if there are more than five measurements for that month. To ensure a continuous time series, it was required that the data record should have at least 3 years of AERONET data measurements, with not less than nine monthly data points for each year during the period from 2000 to 2016.

The data collected was aerosol optical depth (τ). The Angstrom exponent (α) was calculated using Eq. (3). The study covers stations in Nairobi, Skukuza and Ilorin; these stations are ideally placed to study the spatio-temporal distribution of coarse (mineral dust) and fine (biomass burning) particles over the region.

Data Analysis

The level-02 collection-06 terra-MODIS aerosol data (MOD04_L2_C006) and level-02 collection-06 aqua-MODIS aerosol data (MYD04_L2_C006) extracted from the Deep Blue (DB) algorithm in MAPSS website was used in this analysis, from which the long-term (2000 – 2015) daily data was obtained. The daily data was used to compute the monthly and seasonal averages over the entire period of study. The dataset was divided into two groups (rainy and dry seasons) based on the seasonal variations used by Anuforom *et al.*[38]. Validation exercise was then carried out using the monthly mean data of τ_{550} from aqua- and terra-MODIS against AERONET after setting the intercept to zero. In choosing the best MODIS sensor for each station, two parameters were observed. One is the slope (which may suggest an overestimation or underestimation) of the regression analysis, while the other is the coefficient of determination (R^2) which determines the correlation between the two parameters being compared. The large data density for the period makes it easy for the monthly cycle and distribution trends of the parameters to be distinguished. The quantitative analysis of the scatter plots of the $\alpha_{470-660}$ *vs.* τ_{550} was used for classification. The distribution patterns of different aerosols over the stations were equally investigated seasonally.

Using Table 2, the optical properties of aerosols found in the study area were quantitatively identified based on the scatter plots of the $\alpha_{470-660}$ *vs.* τ_{550}. It should be noted that because of the overlap between the discrimination parameters of urban and industrial (UI) aerosol and biomass burning (BB), the combination of the two (UI + BB) will be denoted by urban/industrial and biomass burning (UB) in some classifications. Continental aerosols (CAs) are used to denote aerosols such as sea salts, while desert dust (DD) denotes aerosols emanating from arid or desert areas. The distribution patterns of the different aerosols over the study region for the overall and seasonal data were determined. This method was applied to determine the aerosol types for different months and consequently seasons throughout the years.

TABLE 2. Threshold values of aerosol properties for different types of aerosol adopted in this study area.

Type	α	*vs.*	τ
CA	$\alpha < 0.9$		$\tau < 0.30$
DD	$\alpha < 0.7$		$\tau > 0.40$
BB	$\alpha > 1.0$		$\tau > 0.35$
UI	$\alpha > 1.0$		$\tau > 0.35$

Results and Discussion

Comparisons between τ from the AERONET and MODIS

Figs. 2, 3 and 4 show the correlation plots of both aqua- and terra-MODIS AOD (τ) retrievals against AERONET τ during the years from 2000 to 2015 at the AERONET stations in Nairobi, Skukuza and Ilorin.

Table 3 summarizes the results of the validation of both aqua- and terra-MODIS τ with AERONET τ at the three AERONET stations. It can be observed that aqua-MODIS τ data at Nairobi station, being underestimated, is relatively better compared with AERONET τ than terra-MODIS τ. The station's aqua-MODIS τ had a lower underestimation (29.80 %) than its terra-MODIS counterpart (35.80 %). On the other hand, in Ilorin station, aqua-MODIS τ was overestimated (by 2.90 %), but better compared with AERONET τ than terra-MODIS τ. Conversely, terra-MODIS τ (also being underestimated by 1.90 %) was closely related to its AERONET counterpart at Skukuza station than aqua-MODIS τ.

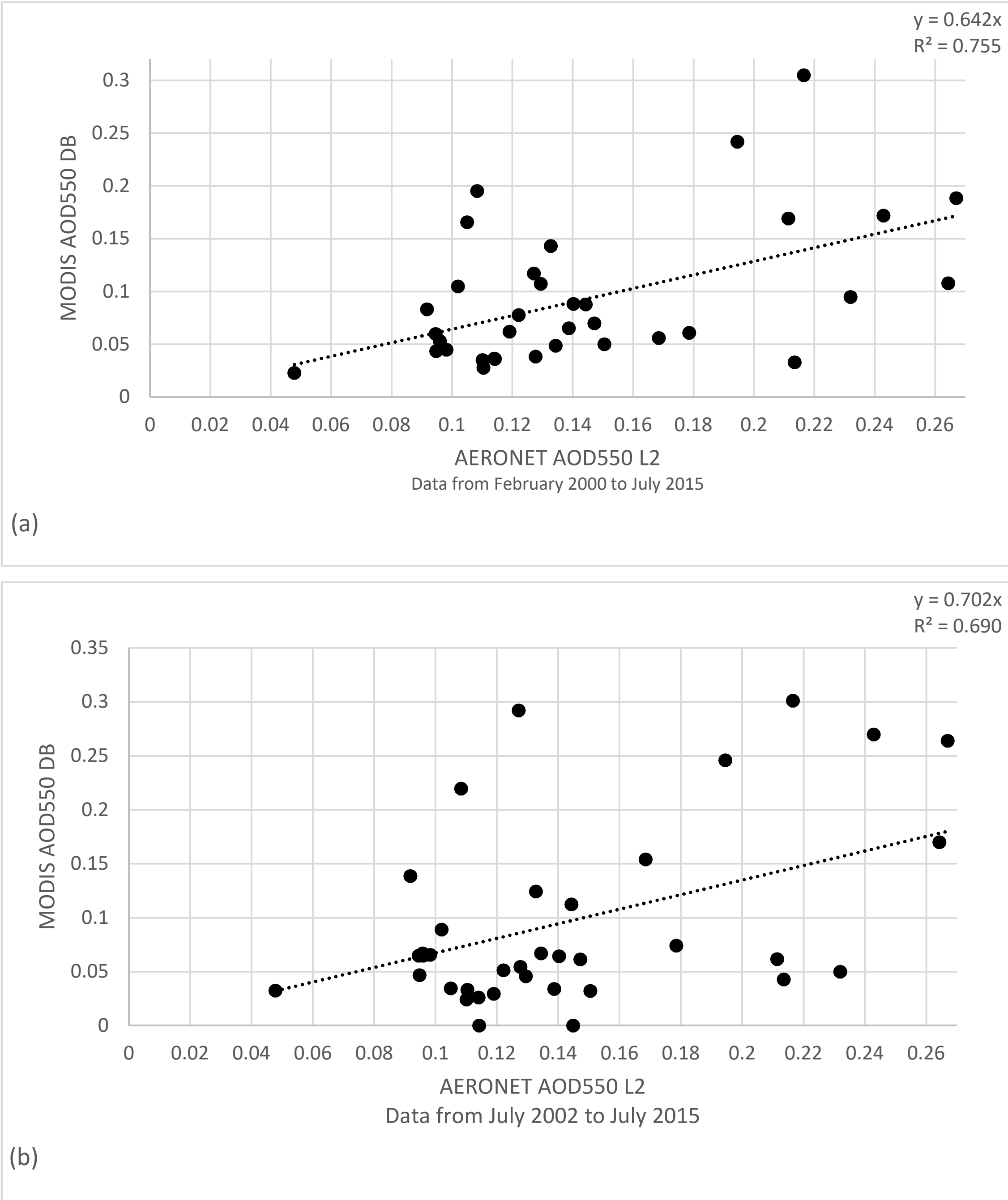

FIG. 2. Comparison of (a) aerosol optical depth (AOD) measured by AERONET and Terra-MODIS and (b) aerosol optical depth (AOD) measured by AERONET and Aqua-MODIS at Nairobi.

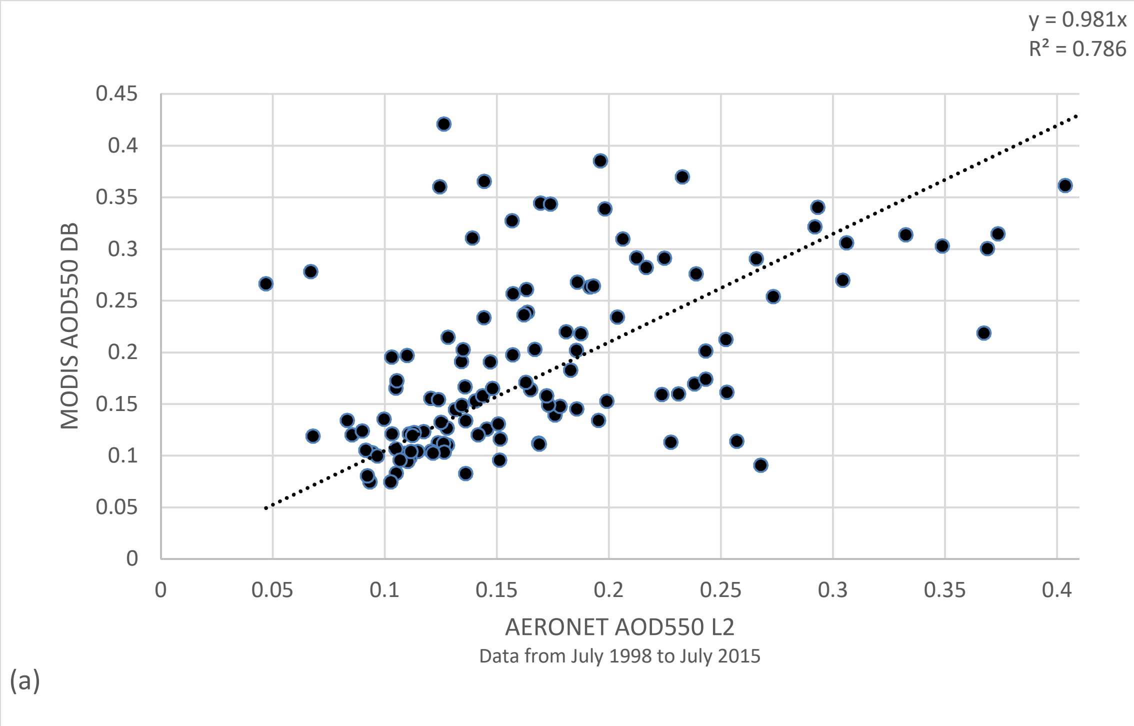

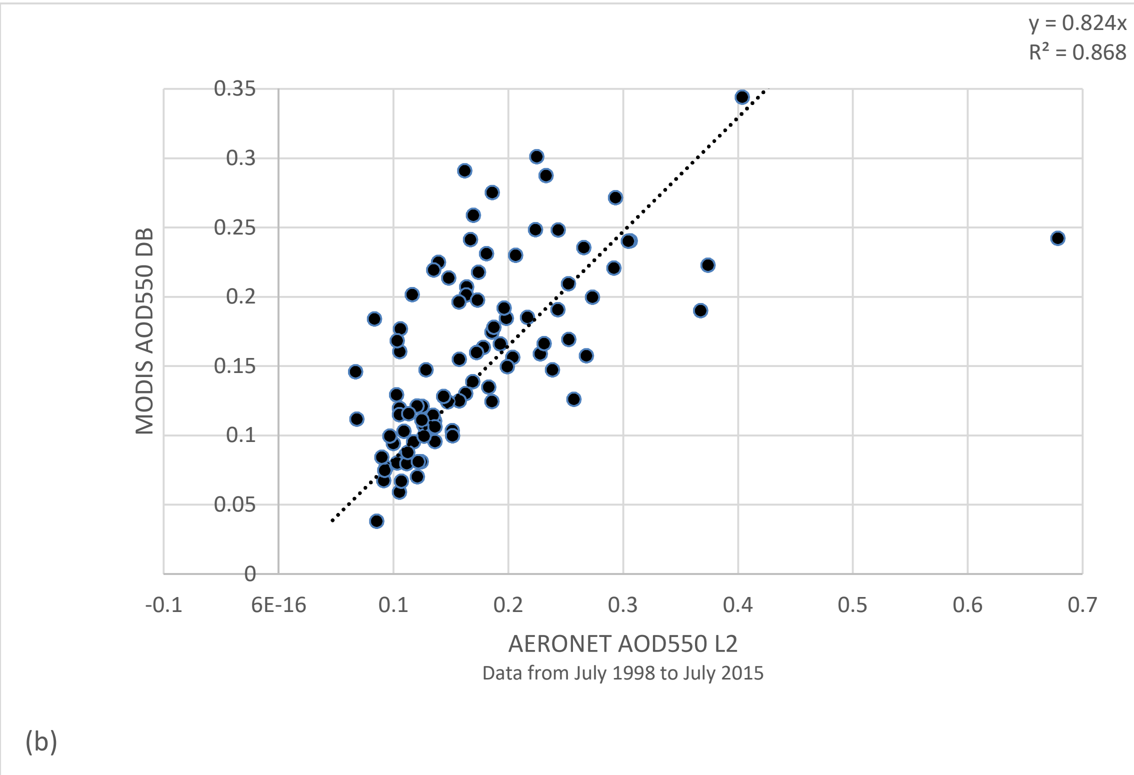

FIG. 3. Comparison of (a) aerosol optical depth (AOD) measured by AERONET and Terra-MODIS and (b) aerosol optical depth (AOD) measured by AERONET and Aqua-MODIS at Skukuza.

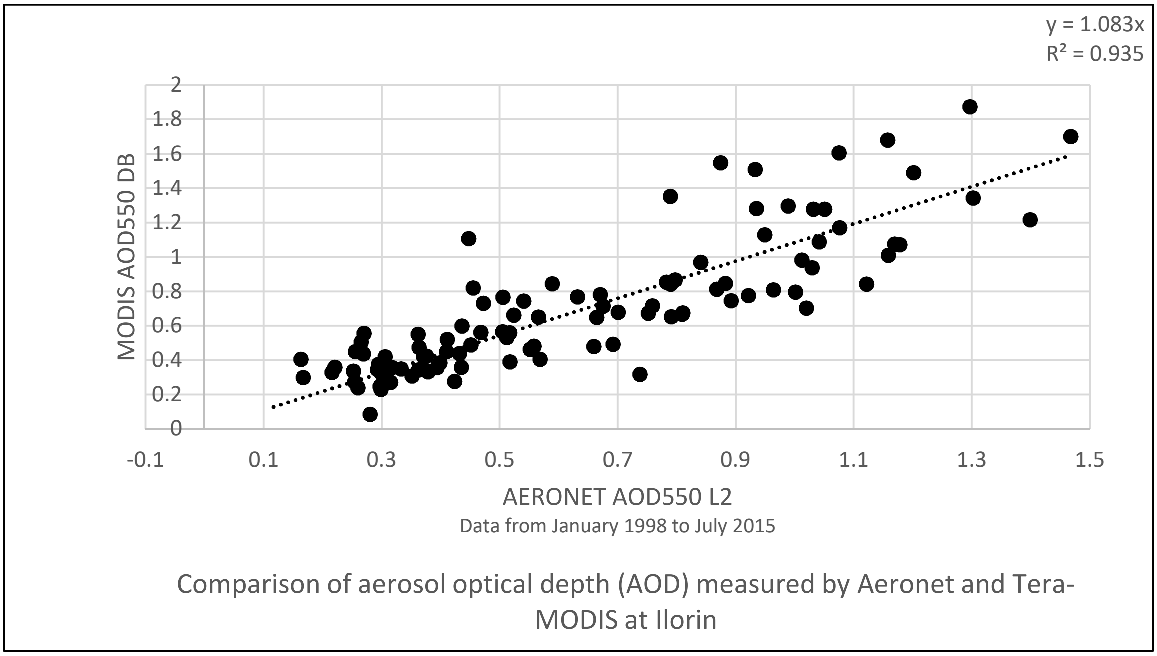

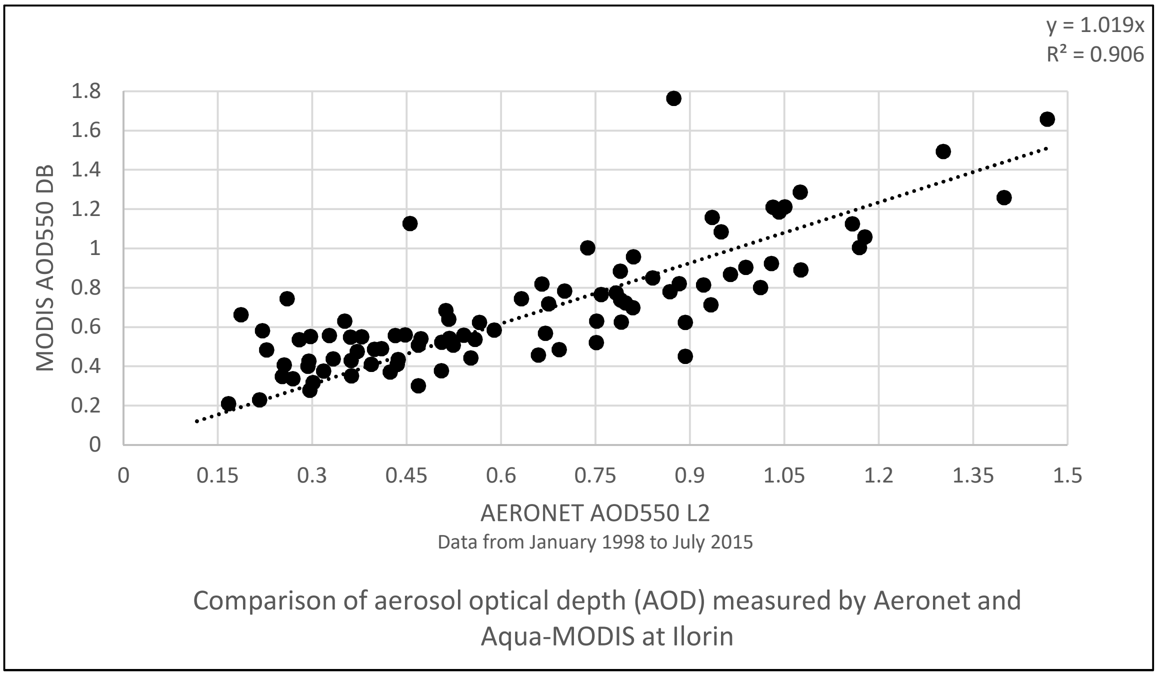

FIG. 4. Comparison of (a) aerosol optical depth (AOD) measured by AERONET and Terra-MODIS and (b) aerosol optical depth (AOD) measured by AERONET and Aqua-MODIS at Ilorin.

TABLE 3. The results of regression analysis for MODIS (aqua and terra) τ *vs*. AERONET τ for the years (2000 – 2015).

	Aqua-MODIS		Terra-MODIS	
Case	Slope	R^2	Slope	R^2
Nairobi	0.702	0.690	0.642	0.755
Skukuza	0.824	0.868	0.981	0.786
Ilorin	1.029	0.930	1.083	0.935

An R^2 (between 0.690 and 0.935) observed for the two MODIS sensors indicates that there is good agreement between MODIS and AERONET data. It also provides confidence that aerosol optical and radiative properties over the study area can be analyzed using MODIS aerosol retrievals.

TABLE 4. The results of regression analysis for MODIS τ *vs*. AERONET τ during each season across the study area for the years (2000 – 2015).

	Dry season		Rainy season	
Case	Slope	R^2	Slope	R^2
Nairobi	0.499	0.878	0.703	0.751
Skukuza	0.818	0.774	0.828	0.948
Ilorin	1.072	0.951	1.134	0.876

Similarly, Table 4 shows the seasonal validation of the best retrievals of MODIS τ *vs*. AERONET τ. It could be seen that MODIS τ had better agreement with AERONET τ during the dry season for only Ilorin station (with overestimation of 7.20 %). On the other hand, Nairobi and Skukuza stations' MODIS τ had better agreement with their AERONET counterpart during the rainy season with an underestimation of 29.70 % and 17.20 %, respectively.

Aerosol Climatology of the Study Area

The monthly mean variations of τ_{550} in the atmosphere measured between February 2000 and July 2015 for the study area are shown in Figure 5. It is evident that the mean monthly τ of Nairobi presents roughly intermediate values with the same trend pattern which are the traits of all low-aerosol loading regions. Nevertheless, the atmosphere in this region is a polluted one (i.e., τ > 0.05). τ values start decreasing in one of the rainy seasons (September to November) and increases significantly during the dry season (January – February). This cycle starts in April, when aerosol concentration begins to build up in the atmosphere; it increases continuously, depicting its peaks in June (a transition month). The month with the highest mean τ is June with a value of 0.17. The month with the lowest mean monthly τ is December (0.047) with a high $\alpha_{470-660}$ value (1.42), indicating the presence of anthropogenic aerosol type. It may be any of biomass burning, urban and industrial aerosols or their combinations. These patterns of monthly cycle of τ (increase after rainy season and decrease after dry season) remain consistent during the 16 years of study. The other rainy season brings about an increase in aerosol load. This may be due to episodes of bush burning at the beginning of the rainy season.

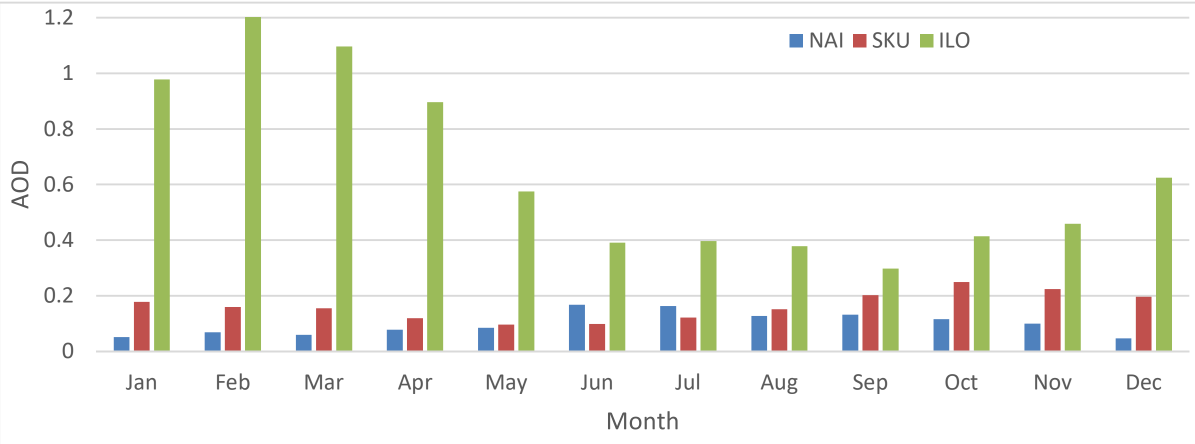

FIG. 5.Monthly mean variations of τ for Nairobi, Skukuza and Ilorin AERONET stations during the study period.

Fig. 5 also shows the variation of the monthly mean τ of Skukuza station and it presents higher values of pollution (though still intermediate). The atmosphere in this region is more polluted than that of Nairobi. The cleanest month is May (0.096). τ values start decreasing in the rainy season (October – May) and increase significantly during the dry season (June – October). The aerosols begin to build up in the atmosphere in June; they increase substantially until reaching their peaks in September (a transition month). The month with the lowest mean monthly τ is May with a high $\alpha_{470-660}$ value, indicating the presence of aerosol types other than dust. It may be any of biomass burning, urban or industrial aerosols or their combinations. These patterns of monthly cycle of τ (increase after rainy season and decrease after dry season) remain prominent throughout the study period.

Additionally, Fig. 5 indicates the monthly mean aerosol loading pattern in Ilorin station. This station is the most polluted among the three stations. Its cleanest month is September (0.30). τ values start decreasing in the rainy season (March – September) and increase significantly during the dry season (November – February). This cycle starts in October, when aerosol concentration begins to build up in the atmosphere; it increases continuously until reaching its peak in February. The month with the highest mean monthly τ is February with a low $\alpha_{470-660}$ value, indicating the presence of natural aerosol types. It may be any of maritime, biogenic, mineral dust or their combinations. This pattern of monthly cycle of τ (increase after rainy season and decrease after dry season) was observed throughout the study period.

The τ values in Ilorin may be explained by the fact that it is located in a region where dust aerosol is a regular phenomenon. Only Nairobi station, out of the three stations under study, can be said to have a fairly good air quality all year round for having the minimum monthly τ_{550} of 0.047. According to [39], the average τ values under clean background condition should be less than 0.05.

The mean monthly variations of $\alpha_{470-660}$ in the atmosphere measured between February 2000 and July 2015 for the study area are shown in Fig. 6. It is evident that the observed seasonal pattern in Nairobi can be associated with a high concentration of fine mode (anthropogenic) aerosols all through the seasons. The observed high $\alpha_{470-660}$ values, 1.36 (the least) in February to 1.51 (the highest) in June, are signatures of anthropogenic aerosols, which could be associated with biomass burning, urban and industrial aerosols, or a mixture of the aforementioned. The seasonal dependence of τ has resulted in the corresponding seasonal feature of α discussed below. The lowest value of mean $\alpha_{470-660}$ observed in February is a signature of fine-mode aerosols. It increases until its peak is reached in June. Due to frequent rainfall (September – November), a significant amount of the larger particles is washed down from the atmosphere. $\alpha_{470-660}$ remains considerably high in August and maintains a slight dip in values in September before another rise in October, followed by another dip in February. South-westerly trade wind comes with rain, a consequence of which a significant amount of aerosol is being removed from the atmosphere and deposited on the ground. This natural phenomenon causes the $\alpha_{470-660}$ to become large, even during rainy season.

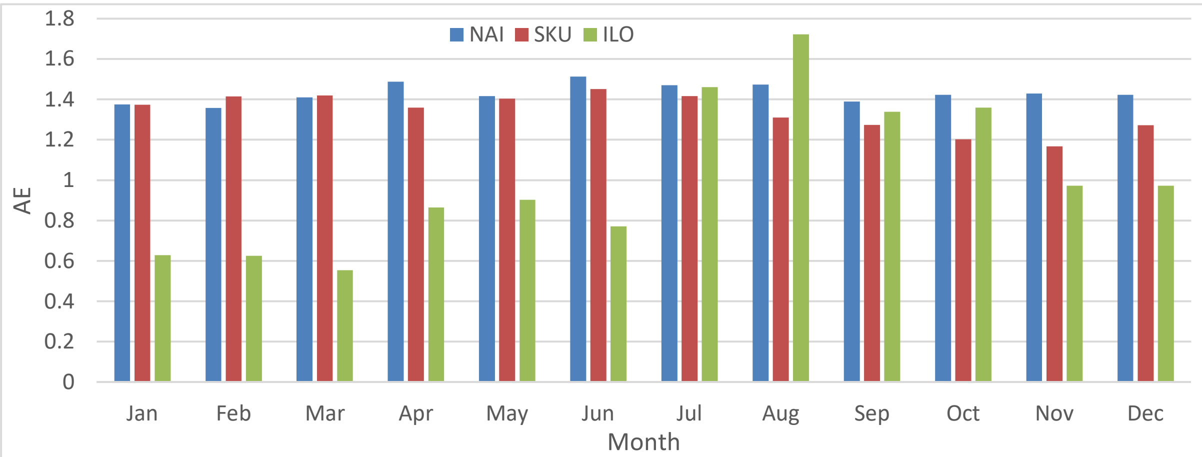

FIG. 6.Monthly mean variations of α for Nairobi, Skukuza and Ilorin AEERONET stations for the study period.

In addition, Fig. 6 shows that the observed seasonal pattern of $\alpha_{470-660}$ in Skukuza can be associated with fairly moderate concentrations of fine-mode aerosols during the dry season. Similar conclusion was drawn by [19] and is supported by our observed low $\alpha_{470-660}$ values, 1.17 in November to 1.45 in June. The values of the mean $\alpha_{470-660}$ observed in the station are signatures of fine-mode particles. It increases from June until the peak is reached in November due to large and frequent rainfall as a result of which a significant amount of the larger particles is washed down from the atmosphere. $\alpha_{470-660}$ remains considerably high in July and maintains a slight dip in values between August and November before another rise in December. Precipitation brings about a significant reduction in the amount of coarse-mode aerosols being removed from the atmosphere.

The observed seasonal pattern for Ilorin station (see Fig. (6)) can be associated with fairly moderate concentrations of coarse-mode aerosols during dry season and fine-mode aerosols during rainy season. Similar conclusion was drawn by [19] and is supported by our observed low $\alpha_{470\text{-}660}$ values, 0.56 in March to 1.72 in August. The transport of dust aerosol from the Sahara to the station by northeasterly dry wind during dry season has been reported by [40]. The lowest value of mean $\alpha_{470\text{-}660}$ observed in March is a signature of mineral dust [41]. It increases from June until the peak is reached in August due to large and frequent rainfall as a result of which a significant amount of larger particles is washed down from the atmosphere. $\alpha_{470\text{-}660}$ remains considerably high in September and maintains a slight dip in values in November, followed by an increment in April. A significant amount of coarse-mode aerosols is being removed from the atmosphere as a result of precipitation during rainy season.

Discrimination of Aerosol Types

This analytical discrimination of aerosol types usually requires knowledge about the optical and physical properties that depend on the wavelength. The parameters employed for this discrimination correspond to the descriptive properties of aerosol loading (τ_{550}) and aerosol size ($\alpha_{470\text{-}660}$) and this is the most used aerosol discrimination method [20,29,34,42,43,44,45]. To effectively characterize and classify different aerosol types in the sub-Saharan Africa, the threshold criteria provided by Kannemadugu *et al.*[20] were adopted for this work. A lot of literature discussed different aerosol classes, like desert dust (DD), continental aerosol (CA), Urban and Biomass burning aerosol (UB) and Mixed-type aerosol (MT). According to Kannemadugu *et al.*[20], the size distributions are dominated by CA when $\tau_{550} < 0.3$ and $\alpha_{470\text{-}660} < 0.9$. For UB, $\tau_{550} > 0.35$ with $\alpha_{470\text{-}660} > 1.0$, while DD is represented by a $\tau_{550} > 0.4$ and $\alpha_{470\text{-}660} < 0.7$. It should be noted that because of the overlap between the discrimination parameters of urban and industrial (UI) aerosol and biomass burning (BB), the combination of the two (UI + BB) will be denoted by urban/industrial and biomass burning (UB) in some classifications.

The scatter plots of Figs. 7 (a – c) were analyzed. It was established that different types of aerosols are present in this station. It is obvious from the plots that α shows increasing values with increasing τ, which indicates the presence of fine-mode particles. Also observed is the wide range of values of α (between 0.75 and 1.70) at low τ ($\leq$0.40) during rainy season, indicating the presence of different aerosol types under relatively clear atmospheric conditions. Also, the highest number of measurements in the scatter plots for this site is concentrated in the area corresponding to $\alpha_{470\text{-}660}$ (1.20 – 1.60) and τ between 0.00 and 0.15, indicating the presence of biomass burning, urban and industrial aerosols. Aerosols from CA and UB with large number of MT are observed in this cluster. Yet, the area corresponding to MT has a very large number of measurements compared to others. This is likely due to the mixing of CA and UB in the atmosphere [39], as well as the absorption of moisture by these aerosols. The CA noticed during rainy season could be as a result of sea salt transport from the Atlantic Ocean, while UB may be as a result of transport sector emissions, biomass burning or urban and industrial aerosol injection events. There are also large numbers of measurements concentrated at $\tau < 0.15$, which are characterized by $\alpha_{470\text{-}660} > 1.00$. This is also a case of strong transport sector emission, biomass burning or urban and industrial aerosol injection events. The study further notes similar patterns of aerosol distribution during dry and rainy seasons (Figs. 7 (b) and 7 (c)). MT and UB were noticed during dry season, while CA and MT were present during rainy season.

The relative frequencies of these aerosols are shown in Fig. 8. The MT class was determined as the highest frequency of occurrence (98.33%) in the overall data. This is likely due to the mixture of DD, CA and UB in the atmosphere. The next highest was the UB class (1.11%) and could be as a result of the injection of biomass burning aerosols and those from urban and industrial aerosol injection events. CA is the next most important in this region and it accounts for 0.56% of its aerosol loading. This may be a result of aerosol transport from the Atlantic Ocean. DD aerosol is not present in this station.

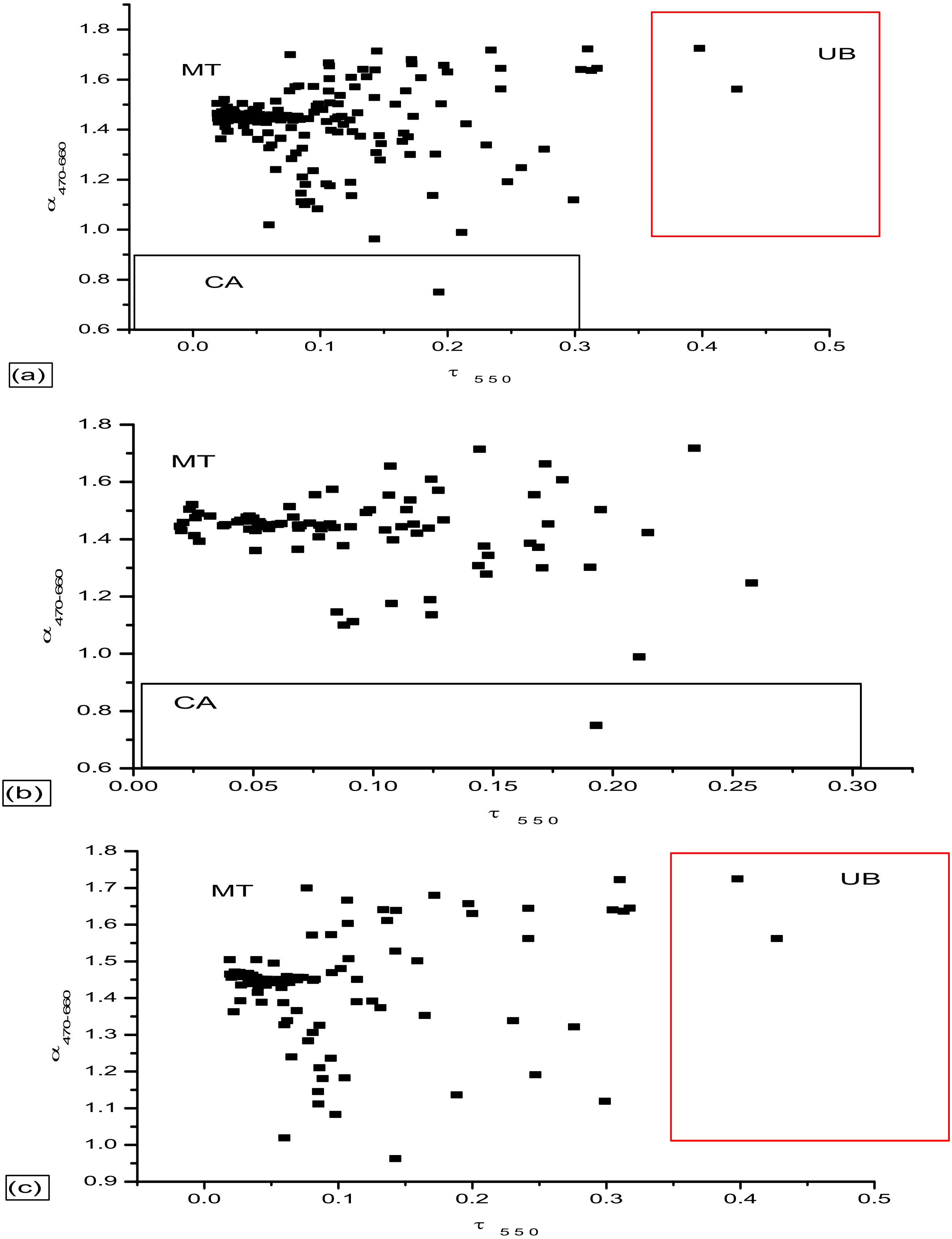

FIG. 7. Scatter plot between τ_{550} and $\alpha_{470\text{-}660}$ for determining the diverse aerosol types generally and for each season over Nairobi ((a) Overall; (b) Rainy season; (c) Dry season).

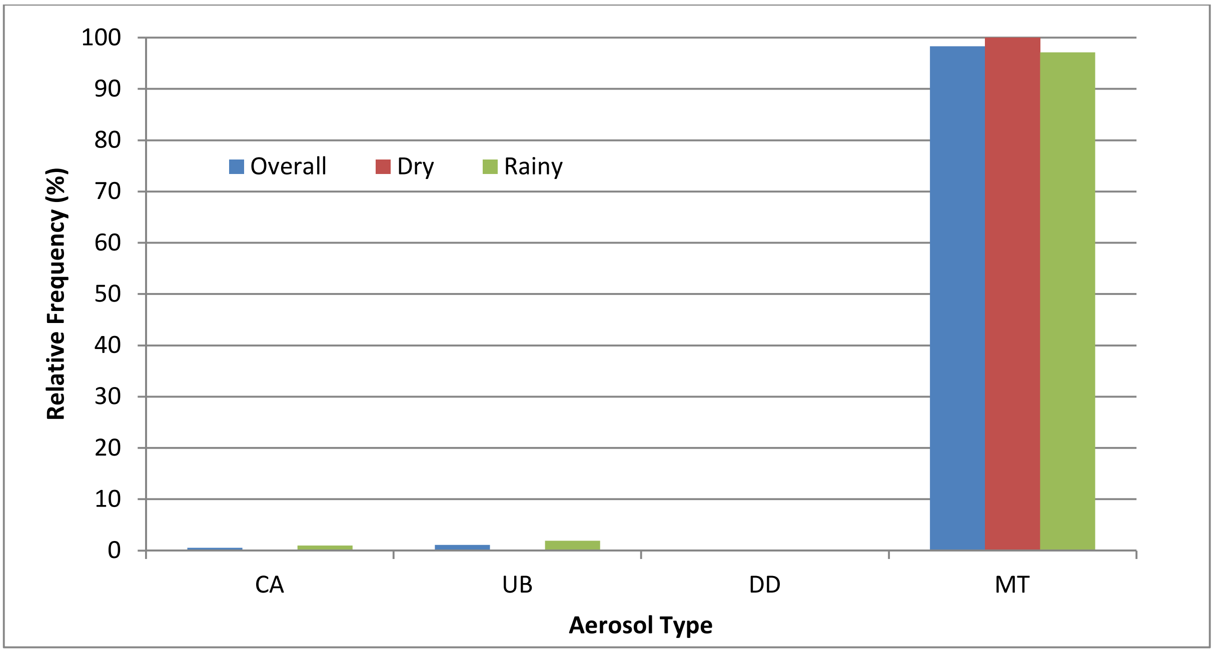

FIG. 8. Percentage contributions of various aerosol types derived from $\alpha_{470\text{-}660} - \tau_{550}$ scatter plots for Nairobi.

The same Figure shows that the frequency of aerosol distribution in the station is not dependent on seasonal change. MT aerosols were dominant (100.00% and 97.14%) in both seasons (dry and rainy seasons). Just like in Mbita station, this could be related to a large amount of aerosols that cannot be determined. The results also show that no other type of aerosol was captured during dry season. This is clearly a case of mixing of aerosols of different types to change their identity. During rainy season, different aerosol species were found related to the multiple peaks, which can also be clearly seen in Fig. 7 (c), where MT is the most dominant aerosol type. UB (1.91%) is the second most dominant aerosol type in the station and this may be a result of the use of biomass as fuel around the station. CA (0.95%) is the third most important aerosol in the region. This may be attributed to the south-westerly trade wind which transports the marine aerosol from Atlantic Ocean as well as the impact of rainy season. Lastly, DD aerosol type is not present in this station.

Figs. 9 (a – c) show the scatter plots of τ *vs*. α over Skukuza. It can be seen from the plots that α shows increasing values with increasing τ, which indicates the presence of fine-mode particles. Also observed is the wide range of values of α (between 1.00 and 1.70) at low τ ($\leq$0.35) during rainy season, indicating the presence of a single type of aerosol under relatively clear atmospheric conditions. Furthermore, the highest number of measurements in the scatter plots for this site is concentrated in the area corresponding to $\alpha_{470\text{-}660}$ (1.10 – 1.60) and τ between 0.05 and 0.25, indicating the presence of fine-mode particles. Aerosols from UB with large number of MT are observed in this cluster. However, the area corresponding to MT has a very large number of measurements compared to others. There are also large numbers of measurements concentrated at $\tau < 0.25$ which are characterized by $\alpha_{470\text{-}660} > 1.1$. This case corresponds to the occurrence of heavy pollution events of the fine-mode type. The study further notes similar patterns of aerosol distribution during dry and rainy seasons (Figs. 9 (b) and 9 (c)). Only MT was noticed during the rainy season, while UB and MT were present during the dry season.

The relative frequencies of these aerosols are shown in Fig. 10. The MT class was determined as the highest frequency of occurrence (99.36%) in the overall data. This is likely due to the mixture of CA and UB in the atmosphere, as well as the absorption of moisture by these aerosols. The only other aerosol type noticed was the UB class (0.64%), which could be a result of automobile emissions, as well as industrial and biomass burning emissions in the station.

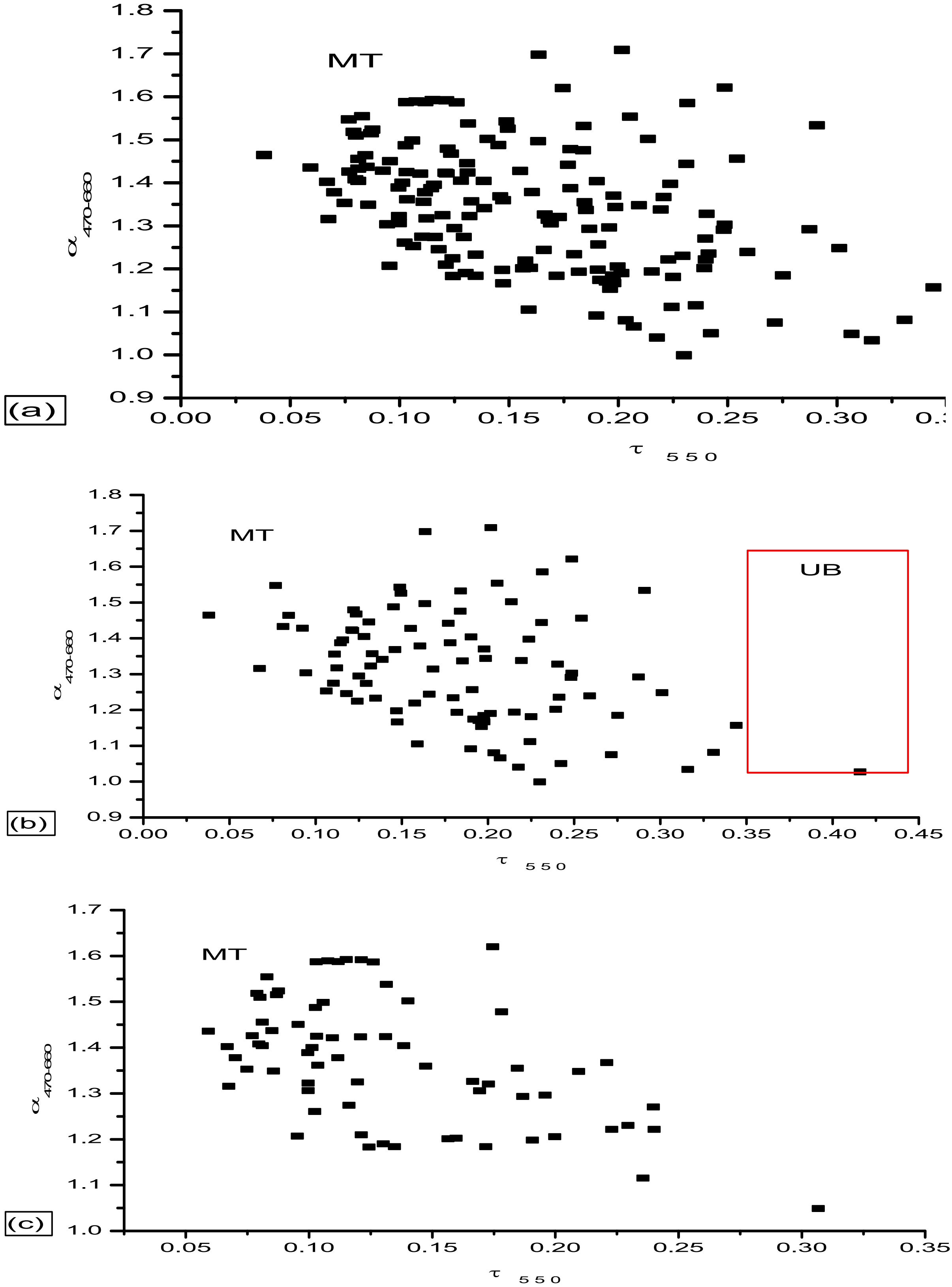

FIG. 9. Scatter plot between τ_{550} and $\alpha_{470\text{-}660}$ for determining the diverse aerosol types generally and for each season over Skukuza ((a) Overall; (b) Rainy season; (c) Dry season).

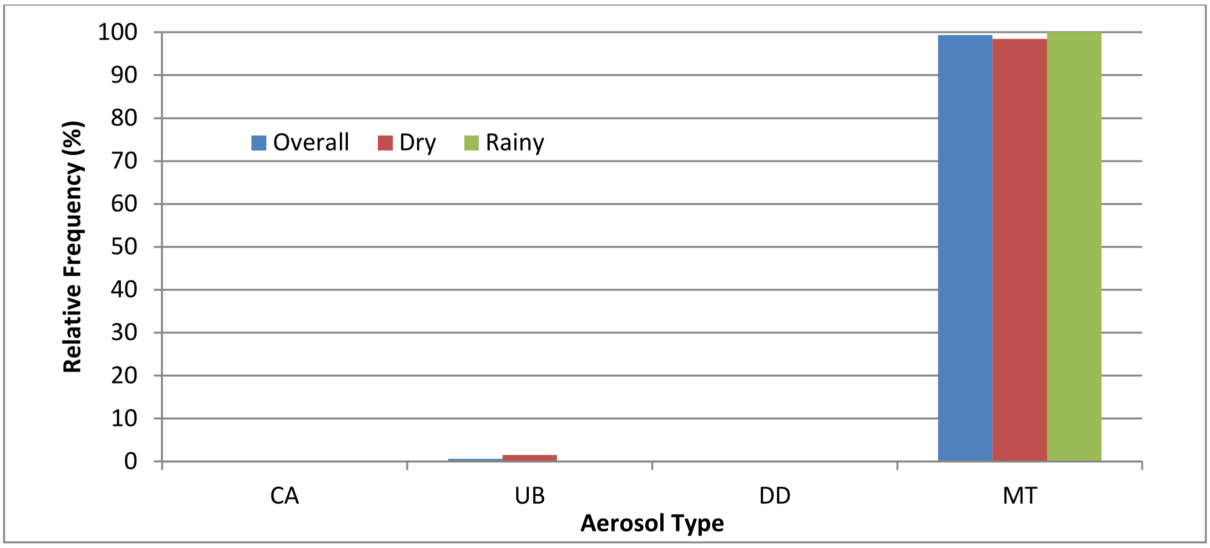

FIG. 10. Percentage contributions of various aerosol types derived from $\alpha_{470\text{-}660} - \tau_{550}$ scatter plots for Skukuza.

From the evidence in Figs. 9 (b) and 9 (c), the MT aerosol type is dominant (98.46% and 100.00%) in both seasons (dry and rainy seasons). This could be related to a large amount of aerosols that cannot be determined; i.e., mixed type (MT) which signifies the occurrence of different aerosol species. During both dry and rainy seasons, UB (1.54% and 0.64%) was the second and the last aerosol type discovered at the station.

Using the criteria, the scatter plots of Figs. 11 (a – c) were analyzed. It is clear from the plots that α shows decreasing values with increasing τ, which indicates the presence of coarse-mode particles, mostly dust [46]. This may be connected with the transportation of dust from construction sites and the Sahara desert into the station. Also observed was the wide range of values of α at low τ (≤0.8) during rainy season, indicating the presence of different aerosol types under relatively clear atmospheric conditions. Furthermore, the highest number of measurements in the scatter plots for this site is concentrated in the area corresponding to $\alpha_{470\text{-}660}$ (0.20 – 1.50) and τ between 0.20 and 1.00, indicating the presence of both anthropogenic and natural particles. Aerosols from CA, DD and UB with large number of MT are observed in this cluster. However, the area corresponding to MT has a slightly larger number of measurements compared to others. There are also large numbers of measurements concentrated at $\tau < 1.20$, which are characterized by $\alpha_{470\text{-}660} < 1.40$. This case corresponds to the occurrence of strong dust activities and heavy pollution events of biomass burning and urban and industrial aerosols. The study further notes similar patterns of aerosol distribution during dry and rainy seasons (Figs. 11 (b) and 11 (c)). Only UB, DD and MT were noticed during the dry season, while CA, DD, UB and MT were present during the rainy season.

The relative frequencies of these aerosols are shown in Fig. 12. The MT class was determined as the highest frequency of occurrence (38.61%) in the overall data. The next highest was the DD class (33.54%) and could be a result of the geographic location of the station. UB is the next most important in this region and it accounts for 23.32% of its aerosol loading. The least important class of aerosol in terms of pollution in this station is UB (2.53%).

With respect to the adopted classification, DD (48.68%) was dominant in the dry season. This is followed by MT and UB with relative frequency values of 32.90% and 18.42%, respectively.

During rainy season, MT (44.44%) was the most dominant aerosol type. This may be attributed to a mix of all or some of the aerosol types in the station, as well as the absorption of water vapour by the aerosols. UB (32.10%) is the second most dominant aerosol type and this may be due to the increase in biomass burning for warming up homes and cooking during the coolness occasioned by the rainy season. DD (18.52%) is the third most important aerosol. This may be attributed to the washing away of dust by rain. Lastly, CA (4.94%) is the least dominant aerosol type.

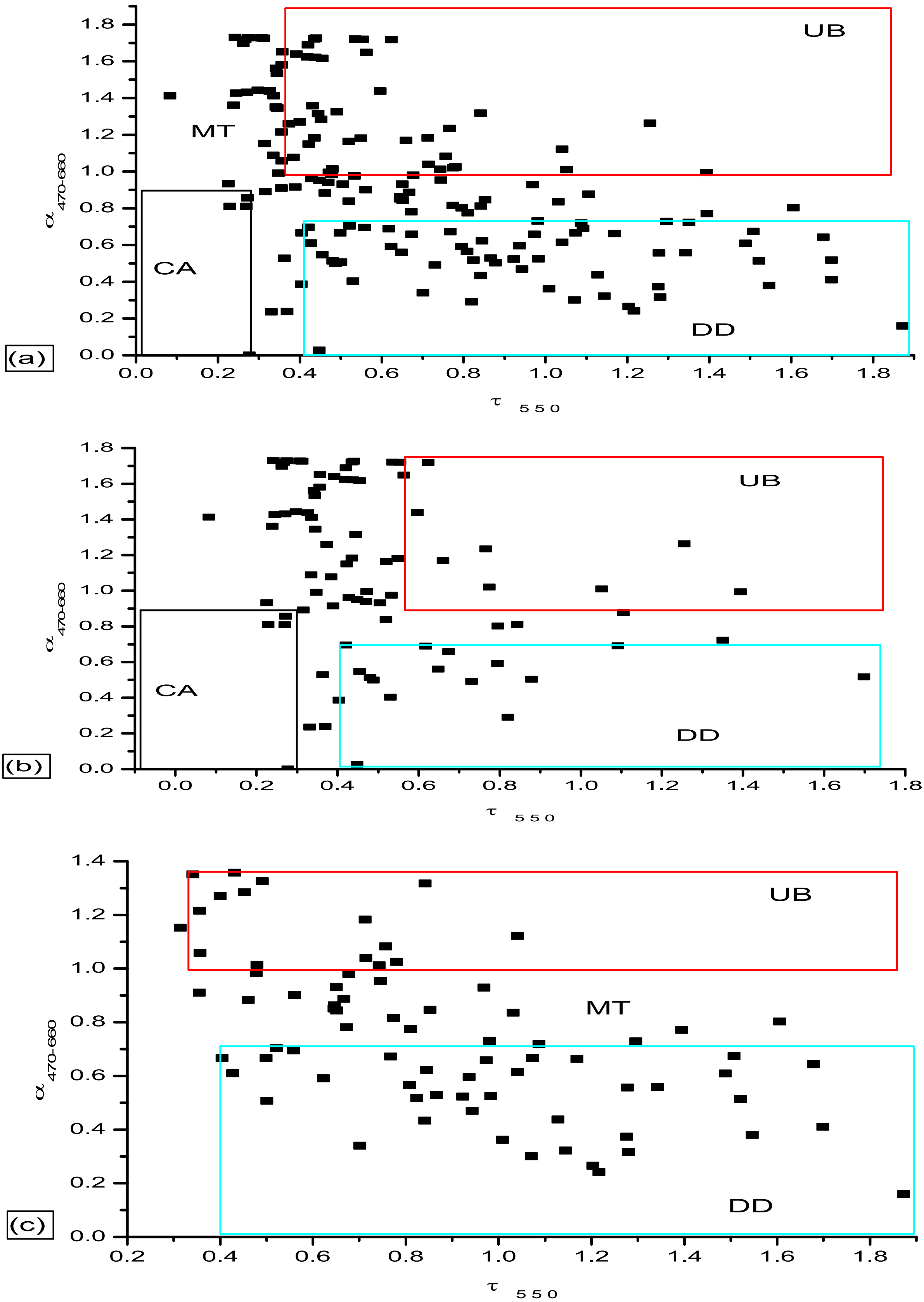

FIG. 11. Scatter plot between τ_{550} and $\alpha_{470\text{-}660}$ for determining the diverse aerosol types generally and for each season over Ilorin ((a) Overall; (b) Rainy season; (c) Dry season).

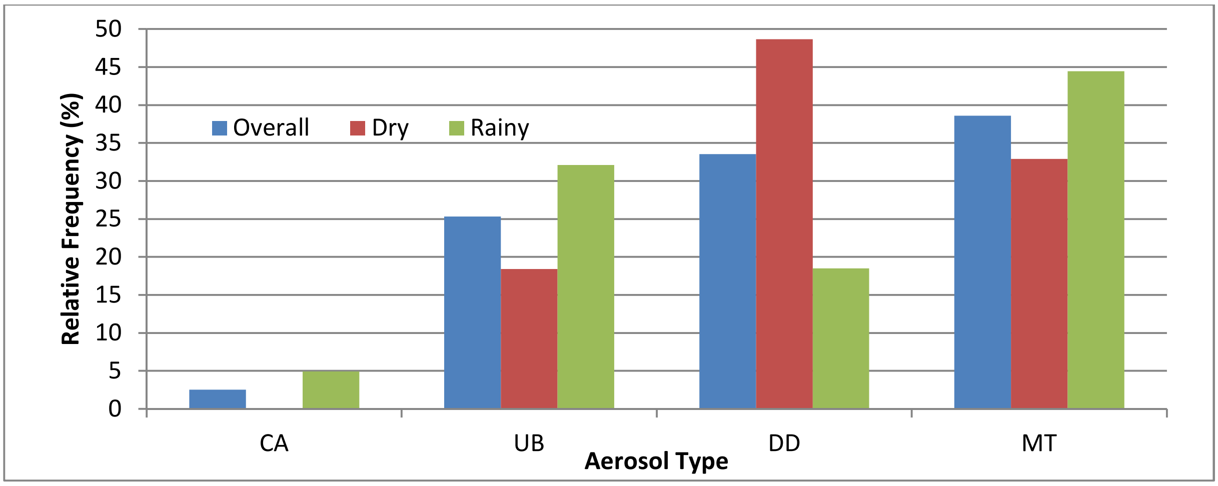

FIG. 12. Percentage contributions of various aerosol types derived from $\alpha_{470\text{-}660} - \tau_{550}$ scatter plots for Ilorin.

The result of the analysis of monthly distribution of aerosol types is presented in Fig. 13. The result obtained for Nairobi (Fig. 13 (a)) shows that the aerosols in the station are homogeneous (i.e., predominantly MT). The dominance of MT aerosols suggests that the atmospheric condition in Nairobi will be a blend of the characteristics of all the aggregate aerosols. There are 7.14% of CA in May and 12.50% of UB in June, while the rest are MT. May is expected to be cool because of the presence of CA (scattering atmosphere), while June is expected to be warm because of the presence of UB (heated atmosphere).

Yet again, the result obtained for Skukuza (Fig. 13 (b)) shows that the aerosol in the station is homogeneously MT aside 7.69% of UB in November. MT aerosols' predominance in Skukuza suggests that the atmospheric condition will also be a blend of the characteristics of all the aggregate aerosols. November is expected to be warmer than other months because of the presence of UB.

In conclusion, results obtained in Ilorin (Fig. 13 (c)) shows that each month has a minimum of two aerosol types. The months of January through April are expected to be cool, because DD is the predominant type of the aerosols found in those months. May, July and November are expected to be warmer, while June, August, September, October and December are expected to be a blend of the characteristics of the predominant aerosols. It was noted that CA's presence was only during some rainy season months, UB and MT's presence cut across both seasons, while DD's presence was noted during the dry season and the early part of the rainy season. UB aerosols are associated with bush and refuse burning as well as exhaust from automobiles and factories. CA can be associated with smaller number of observations as a result of cloud interactions.

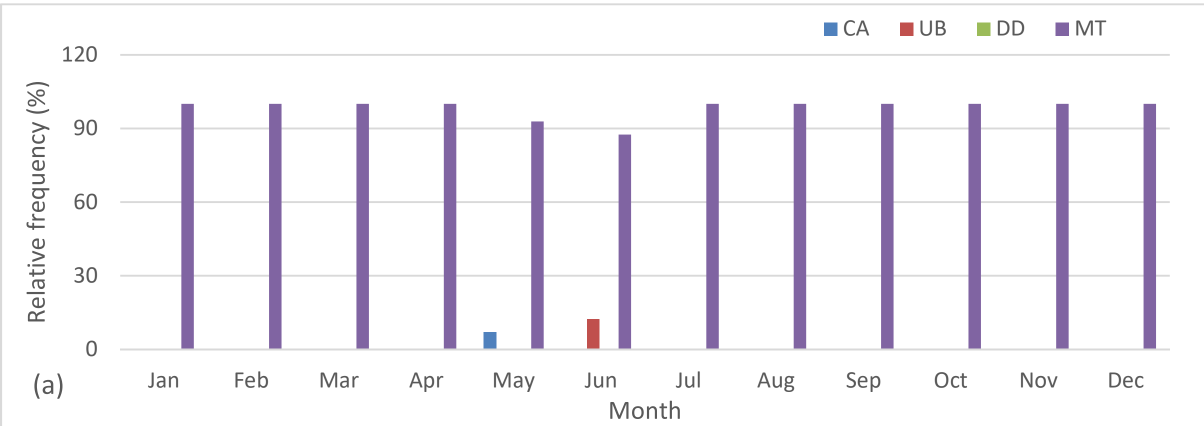

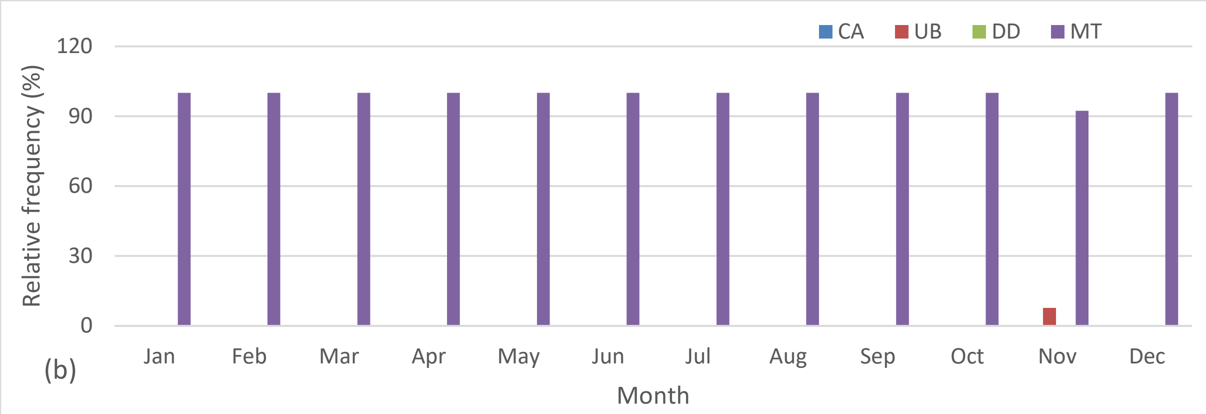

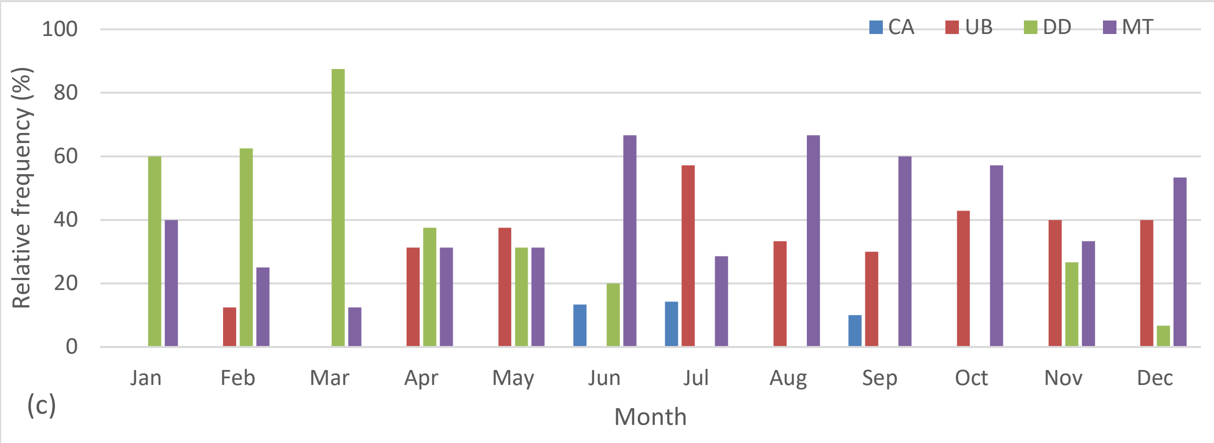

FIG. 13. Percentage contributions of various aerosol types derived from monthly $\alpha_{470\text{-}660} - \tau_{550}$ scatter plots over (a) Nairobi, (b) Skukuza and (c) Ilorin.

Conclusion

In this work, an attempt was made to analyze the temporal variation of aerosol optical depth (τ) and Angstrom exponent (α) for the period from February 2000 to July 2015 over Nairobi, Skukuza and Ilorin AERONET stations. Validation of aqua- and terra-MODIS τ with AERONET τ was carried out. The overall validation shows that terra-MODIS τ was better than the aqua-MODIS counterpart in Skukuza because of its lower underestimation when compared with aqua-MODIS. Similarly, aqua-MODIS τ was better than its terra-counterpart at Nairobi and Ilorin stations. The coefficient of determination (R^2) for both validations ranges from 0.690 to 0.935. On seasonal bases, the underestimation during rainy season was better at Nairobi and Skukuza stations, while Ilorin station shows a better overestimation during dry season. The R^2 value for both seasons was found to be between 0.751 and 0.951.

The τ *vs.* α method employed for the discrimination of aerosols showed an obvious domination of MT aerosols (98.33 %) overall in Nairobi station, while the next highest contributor comes from the UB aerosol type (1.11 %) and CA (0.56 %) in Nairobi station. The result was similar during dry and rainy seasons. At Skukuza station, the dominant aerosol overall and throughout the dry and rainy seasons was MT aerosols (99.36 %, 98.46 % and 100.00 %, respectively), followed by an insignificant amount of UB aerosols (0.64 %). During dry season, UB aerosols (1.54 %) were the only other aerosol type present. At Ilorin station, MT aerosol type (38.61 %) was dominant overall and DD (33.54 %) was second highest followed by UB (25.32 %) and CA (2.53 %). During the dry season, DD (48.68 %) was the dominant aerosol type, followed by MT (32.90 %) and UB (18.42 %), whereas MT (44.44 %), UB (32.10 %), DD (18.52 %) and CA (4.94 %) were present during the rainy season.

Acknowledgement

The authors wish to thank the Principal Investigators (PIs) of AERONET sites and their staff for establishing and maintaining these sites. In addition, the authors would like to thank the Giovanni team for developing and hosting the MAPSS database and the Web MAPSS user interface.

References

[1] Ghan, S.J. and Schwartz, S.E., "Aerosol Properties and Processes: A Path from Field and Laboratory Measurements to Global Climate Models", A report by The U.S. Department of Energy strategy for improving the treatment of aerosol properties and processes in global climate models, (2007).

[2] Mogo, S., Cachorro, V.E., de Frutosa, A. and Rodrigues, A., *J. Environ. Monit.*, 14 (2012) 3174.

[3] Zhang, J. and Reid, J.S., *J. Geophys. Res. Atmos.*, 111 (22) (2006) 1.

[4] Li, Z. *et al.*, *J. Geophys. Res. Atmos.*, 112 (2007) D22S07.

[5] Misra, A., Jayaraman, A. and Ganguly, D., *Aerosol Air Qual. Res.*, 15 (2015) 252.

[6] Chu, D.A., Kaufman, Y.J., Ichoku, C., Remer, L.A., Tanré, D. and Holben, B.N., *Geophys. Res. Lett.*, 29 (12) (2002) 1.

[7] Ichoku, C. *et al.*, *Geophys. Res. Lett.*, 29 (12) (2002) 1.

[8] Levy, R.C. *et al.*, *J. Atmos. Sci.*, 62 (2005) 974.

[9] Kaufman, Y.J., Tanré, D., Remer, L.A., Vermote, E.F., Chu, A. and Holben, B.N., *J. Geophys. Res.*, 102 (D14) (1997) 17051.

[10] Levy, R.C., Remer, L.A., Mattoo, S., Vermote, E.F. and Kaufman,Y.J., *J. Geophys. Res. Atmos.*, 112 (13) (2007) 1.

[11] Hsu, N.C. *et al.*, *IEEE Trans. Geosci. Remote Sens.*, 42 (3) (2004) 23.

[12] Granados-Munoz, M.J. et al., *Proceedings of the Global Conference on Global Warming 2011, 11 - 14 July,Lisbon, Portugal*, (2011), pp. 1–10.

[13] Kaufman, Y.J., Tanré, D. and Boucher, O., *Nature*, 419 (2002) 215.

[14] Remer, L.A. *et al.*, *J. Atmos. Sci.*, 62 (4) (2005) 947.

[15] Yu, H. *et al.*, *J. Geophys. Res. Atmos.*, 114 (10) (2009) 1.

[16] Yu, H. *et al.*, *Science (80-.)*, 337 (6094) (2012) 566.

[17] Bibi, H., Alam, K. and Bibi, S., *Atmos. Res.*, 181 (4) (2016) 106.

[18] Szkop, A., Pietruczuk, A. and Posyniak, M., *Acta Geophys.*, 64 (6) (2016) 2650.

[19] Kaskaoutis, D.G., Kambezidis, H.D., Hatzianastassiou, N., Kosmopoulos, P.G. and Badarinath, K.V.S., *Atmos. Chem. Phys. Discuss.*, (2007) 6357.

[20] Kannemadugu, H.B.S., Varghese, A.O., Mukkara, S.R., Joshi, A.K. and Moharil, S.V., *Aerosol Air Qual. Res.*, 15 (2) (2015) 682.

[21] Xin, J. *et al.*, *J. Geophys. Res. Atmos.*, 112 (5) (2007) D05203.

[22] Mbourou, G.N., Bertrand, J.J. and Nicholson, S.E., *J. Appl. Meteorol.*, 36 (1997) 868.

[23] Makokha, J.W., Angeyo, H.K. and Muthama, J.N., *Int. J. Sci. Technoledge*, 5 (3) (2017) 166.

[24] Levy, R.C., Remer, L.A. and Dubovik, O., *J. Geophys. Res. Atmos.*,112 (13) (2007).

[25] Laakso, L. *et al.*, *Atmos. Chem. Phys.*, 12 (2012) 1847.

[26] Tiwari, S. and Singh, A.K., *Aerosol Air Qual. Res.*, 13 (2) (2013) 627.

[27] Ichoku, L.R.C., Kaufman, Y.J. and Remer, L.A., *Adv. Sp. Res.*, 34 (2004) 820.

[28] Holben, B.N., Eck, T.F., Slutsker, I., Tanre´, D., Buis, J.P., Setzer, A., Vermote, E., Reagan, J.A., Kaufman, Y.J., Nakajima, T., Lavenu, F., Jankowiak, I. and Smirnov, A., *Remote Sens. Environ.*, 66 (1998) 1.

[29] Al-Salihi, A.M., *Arab. J. Geosci.*, 11 (633) (2018) 1.

[30] Petrenko, M., Ichoku, C. and Leptoukh, G., *Atmos. Meas. Tech.*, 5 (2012) 913.

[31] Boersma, K.F. and de Vroom, J.P., *J. Geophys. Res. Atmos.*, 111 (20) (2006) 1.

[32] Kumar, K.R. *et al.*, *Atmos. Environ.*, 95 (2014) 400.

[33] Tijjani, B.I., Aliyu, A. and Sha'aibu, F., *Open J. Appl. Sci.*, 4 (2014) 399.

[34] Tan, F., Lim, H.S., Abdullah, K., Yoon, T.L. and Holben, B.N., *Atmos. Pollut. Res.*, 6 (2015) 682.

[35] Eck, T.F. *et al.*, *J. Geophys. Res. D Atmos.*, 104 (1) (1999) 31, 333.

[36] Tijjani, B.I. and Akpootu, D.O., *Int. J. Res. Rev. Pharm. Appl. Sci.*, 2 (6) (2012) 1128.

[37] He, L., Wang, L., Lin, A., Zhang, M., Bilal, M. and Tao, M., *Remote Sens.*, 9 (746) (2017) 1.

[38] Anuforom, A.C., Akeh, L.E., Okeke, P.N. and Opara, F.E., *Atmos. Environ.*, 41 (7) (2007) 1550.

[39] Toledano, C. *et al.*, *Q. J. R. Meteorol. Soc.*, 133 (2007) 795.

[40] Balarabe, M., Abdullah, K. and Nawawi, M., *Atmosphere (Basel)*, 6 (2015) 1462.

[41] Ogunjobi, K., Ajayi, V., Balogun, I., Omotosho, J. and He, Z., *Theor. Appl. Climatol.*, 93 (1–2) (2008) 91.

[42] Sharma, M., Kaskaoutis, D.G., Singh, R.P. and Singh, S., *Aerosol Air Qual. Res.*, 14 (2014) 608.

[43] Kumar, K.R., Sivakumar, V., Reddy, R.R., Gopal, K.R. and Adesina, A.J., *Aerosol Air Qual. Res.*, 14 (2014) 108.

[44] Verma, S., Prakash, D., Ricaud, P., Payra, S., Attié, J. and Soni, M., *Aerosol Air Qual. Res.*, 15 (2015) 985.

[45] Tariq, S., Zia, U.-H. and Ali, M., *Asia-Pacific J. Atmos. Sci.*, 52 (1) (2016) 25.

[46] Ogunjobi, K.O., He, Z., Kim, K.W. and Kim, Y.J., *Atmos. Environ.*, 38 (9) (2004) 1313.